Electrochemical Materials and Technologies

ARTICLE

Electrochemical Materials and Technologies

eISSN: 2949-0561

Cite this: Electrochem. Mater. Technol. 2 (2023) 20232023

Molecular dynamics simulation of the Ni – FLiNaK interface: adsorption layers as origin of metal passivity

Dmitry Zakiryanov [a]*, Mikhail Kobelev [a]

Received: 8 September 2023
Accepted: 31 October 2023
Published online: 10 November 2023

DOI: 10.15826/elmattech.2023.2.023

The method of classical molecular dynamics was used to study the Ni (solid) – FliNaK (melt) phase separation boundary at temperatures of 800 K, 1000K , and 1200 K. An *ab initio*-based pairwise model is developed to describe the interactions that take place at the Ni – FLiNaK interface. It was shown that at temperatures of 800 K and 1000 K, lithium and fluorine ions are predominantly adsorbed on the nickel surface in the form of a two-dimensional ordered structure. Such a dense layer prevents the dissolution of nickel and the metal solid has no defects in the surface layer. However, at a temperature of 1200 K the structure of the adsorption layer is noticeably disturbed with the partial replacement of lithium ions by sodium ones. Along with higher temperature, this leads to the formation of point defects and degradation of the surface layers of the nickel crystal lattice.

keywords: FLiNaK, double layer, molecular dynamics, passivation, adsorption

1. Introduction

The issue of the stability of structural materials in aggressive environments arises in the implementation of numerous technological processes. Nickel and nickel-based alloys are the materials that exhibit high corrosion resistance to molten alkali metal fluorides and chlorides, as well as their mixtures [1, 2].

One of the possible passivation mechanisms is the formation of stable layers on the metal surface, which prevents the metal from entering the melt. Such layers can be formed either in the outer layers of the metal surface due to the chemical interaction of the melt components with the metal, or the metal surface can be covered with an adsorption layer consisting of the melt components. In situ experimental methods for studying the formation of passivation layers at metal-melt interfaces are rather difficult to implement due to high temperatures and aggressiveness of fluoride melts. Therefore, computer simulation methods in such cases represent a convenient alternative for studying the processes occurring on metal surfaces in contact with molten salts, especially with a need in describing nanoscale objects [3].

The modeling of the chemical interaction of the metal and melt components can be performed by first-principles methods based on the calculation of the electronic energy. One of the robust methods is the density functional theory (DFT) [4]. These techniques, using modern computing resources, make it possible to describe objects consisting of several hundred particles. On the other hand, the time scale available in a reasonable computational time is of the order of 10^4 – 10^5 steps. However, if one assumes that the passivation process is based on the physical adsorption of melt components on the metal surface, then in this case the method of classical molecular dynamics will be a convenient tool since it allows increasing both time scale and ensemble size by several orders of magnitude. When considering systems containing tens of thousands of particles over millions of steps, one can not only describe the process of formation

a: Institute of High-Temperature Electrochemistry, Ekaterinburg 620137, Russia

* Corresponding author: dmitryz.ihte@gmail.com

of the surface layer and its structure, but also evaluate the stability of the resulting adsorption layers.

In this study, the molecular dynamics method is used to study a system consisting of solid nickel in contact with a molten eutectic mixture of lithium, sodium, and potassium fluorides (FLiNaK) at various temperatures below the melting point of nickel. The considered heterophase system Ni (solid) – FliNaK (liquid) is a simplified model object. In nature, the fluoride eutectic FLiNaK cannot be completely purified from oxygen impurities, the minimum content of which is several tens of ppm [5]. It is known that oxygen is a surface-active component and is directly involved in adsorption and electrochemical processes on the metal surface [6]. Therefore, the simulation study on the role of oxygen in the mechanism of corrosion of the surface layers of nickel in a fluoride melt can be considered as a promising area of theoretical research. Another important point should be noted is that in our approach all valence states of interacting particles are fixed, i.e. the chemical reactions can not be described. Given that, the main attention in this study will be focused on the distribution of ions near the metal surface and its temperature dependence. Here of great interest is the stability of metal layers which are in contact with the melt.

The aim of this study is to calculate the structural characteristics of the interphase surface for the Ni (solid) – FliNaK (liquid) heterophase system at different temperatures using classical molecular dynamics. The proposed model for describing interactions between metallic nickel and melt components is developed based on *ab initio* energies. To describe the melt, a pairwise model developed in earlier studies is used. When applying the model for simulations of binary mixtures of alkali metal halides [7] and fluoride eutectic (FLiNaK) [8], the calculated structural and transport properties are in good agreement with experimental data.

2. Simulation methods

2.1. Approximations for interactions

The subject of modeling is a multicomponent two-phase metal-melt system, in which its constituent parts have a different nature of the chemical bond. Such diversity inevitably entails the use of several approaches to the description of interparticle interactions. The ionic type of bonding between ions in a fluoride eutectic melt is described via the Born – Meyer pair potential approximation:

$$U_{ij}(r) = \frac{Z_i Z_j e^2}{\varepsilon \cdot r} + A \cdot exp\left[\frac{-r}{\rho}\right], \quad (1)$$

here Z_i is the charge of the i-th ion located at a distance r from the second particle Z_j, ε is the permittivity of the medium (equal to 1 in further calculations), and e is the electron charge. Short-range repulsion parameters A and ρ were obtained earlier [7] on the basis of *ab initio* energies of ion pairs.

The metallic bond in crystalline nickel is described by the EAM (Embedded Atom Model) multiparticle potential, which takes into account not only the interaction of metal atoms with each other, but also with the electronic subsystem. To describe Ni-Ni interaction the consistent set of embedding functions and short-range repulsive pair interaction for face centered cubic (fcc) Ni metal was used [9].

This work is focused on the study of the phase boundary, which means that special attention should be paid to the corresponding metal – melt potentials. To describe the interaction of nickel with ions of the molten fluoride eutectic, we chose the Morse potential:

$$U_{ij}^2(r) = D_e\left(1 - e^{-\alpha(r-r_c)}\right)^2, \quad (2)$$

here r_c is the equilibrium bond distance, D_e is the depth of the well, and α controls the "rigidity" of the potential. Originally developed to describe diatomic molecules [10], this pair potential has also been successfully applied to describe the interaction of particles with surfaces [11]. C. G. Guymon et al. used the Morse potential to describe the interaction of NaCl solution with a copper surface [12]. Their methodology for fitting the potential parameters was close to ours, so we shall discuss it in some more detail. The reference system was a copper surface constructed of 10 atoms with an adsorbed sodium cation, chlorine anion, or water molecule. While energy scans were performed for various distances between the surface and the adsorbed species (z coordinates), the positions of ions and water in the xy plane were strictly predefined by a few symmetry-based sites (moreover, only a single site for sodium). The quality of the fitting to the *ab initio* energies for Na^+ and Cl^- ions was found to be good. This encourages us to rely on the similar reference system.

To obtain the parameters of the Morse potential, we apply first-principle energy calculations. The next section describes the process of fitting the parameters of this potential.

2.2. Fitting of the Morse potential parameters

Potentials were fitted based on *ab initio* calculated interaction energies of metallic Ni with $Li^+/Na^+/K^+/F^-$ ions. The reference system represents a monolayer of nickel atoms above which two melt ions were located in different coordinates (see Figure 1). The interionic

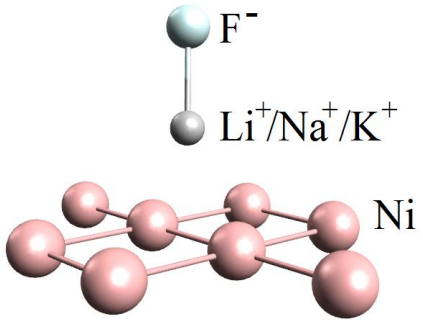

Figure 1 The reference system for calculation of energies.

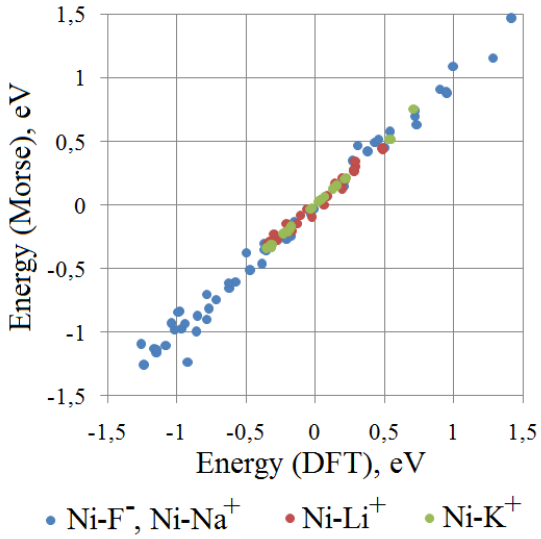

Figure 2 Morse potential fitting results.

Table 1 – The parameters of the Morse potential.

	Ni-F⁻	Ni-Li⁺	Ni-Na⁺	Ni-K⁺
D_e	0.10791	0.14012	0.18516	0.10846
α	1.97166	0.95774	1.06251	0.99485
r_c	1.97081	3.0107	3.24386	3.66957

distance was fixed at the position of the potential energy minimum for that ion pair. The density functional theory with the PBE0 functional [13] was applied. Dispersion interactions are taken into account by means of the Grimme D3 correction [14]. The def2-TZVP [15] basis sets were used.

For each kind of adsorbed pair of ions, the number of configurations was 25. The configurations differed both in the distance to the metal and in the position of the pair of ions in the plane parallel to the plane of the metal. Compared to the study by C. G. Guymon et al. [12], we prefer to set random positions in space to cover not only the symmetry-defined sites, but intermediate positions as well. The pair potential parameters were optimized in order to reproduce changes in energy depending on the system configuration. In all cases, it was possible to achieve good agreement between the reference and model energies, as shown in Figure 2. The highest root-mean-square errors (RMSE) of 0.037 eV are observed for the Ni-Li⁺ pair. The fitted parameters are listed in the Table 1.

2.3. The details of molecular dynamics simulation

The main object of the study is the Ni – FLiNaK interface. Therefore, the following design of the simulated cell, shown in Figure 3, was chosen.

Crystalline nickel with dimensions of 34.5 Å × 53.5 Å × 67.3 Å contains 14080 atoms in a fcc lattice. On both sides of the metal along the *z* axis, there is a fluoride eutectic melt consisting of 13148 ions, which is in contact with the (100) metal faces. Periodic boundary conditions are imposed on the cell in all directions. The system could be interpreted as a 6.73 nm nickel plate surrounded by FLiNaK melt. The parameters of the metal part are chosen in such a way as to prevent the interaction between the liquid phases on both sides of the nickel. Note that in this work it was not supposed to investigate the effect of metal charging on the interface, so there was no need for a second metal electrode.

The fluoride eutectic melt (FLiNaK) was prepared in a separate cell, the geometric parameters of which were chosen in such a way that when combined with crystalline nickel in the *xy* plane, heated to a temperature of 800 K, the linear dimensions of the two phases in the *xy* plane coincided. The cell was assembled from three fragments, as can be seen in Figure 3, (melt | crystalline nickel | melt) and then equilibrated in the NPT ensemble at a temperature of 800 K with the thermostat parameter of 0.1 ps during 1 ns. The pressure was maintained equal to 1 atm. The barostat was anisotropic so the cell relaxation was allowed in all directions independently. After bringing the assembled cell into equilibrium, which was controlled by monitoring the cell volume during the simulation, the barostat conditions were changed to maintain the pressure in an isotropic mode.

The simulation was carried out at temperatures of 800, 1000 and 1200 K, which is higher than the melting point of FLiNaK (727 K), but significantly lower than the melting point of nickel (1728 K). The conditions of constant pressure and temperature were imposed (NPT ensemble). Temperature and pressure control is set using a thermostat and the Nose-Hoover barostat [16]. The temperature relaxation parameter was 0.1 ps, and the analogous parameter for pressure was 0.5 ps.

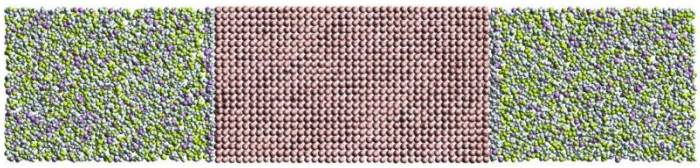

Figure 3 The design of the simulation cell. Here red circles are Ni atoms, while others represent the melt ions.

The pressure in all calculations was 1 atm. The simulation time step for all mixtures was 1 fs, and the total simulation time at each temperature was 15 ns. The cutoff parameters for the Born-Mayer and Morse potentials were 15 Å and 5 Å, correspondingly. The Coulomb interaction was treated by the Ewald method. All calculations were carried out in the LAMMPS [17] package using the URAN supercomputer at the IMM UB RAS.

3. Results and discussion

3.1. T = 800 and 1000 K

At temperatures of 800 and 1000 K, at the beginning of the simulation during the first ~100 ps, a compacted layer is formed in the melt near the phase separation interface. This layer contains all the ions that are in the melt, but the main part is lithium cations and fluorine anions. At a temperature of 800 K, after 5 nanoseconds of simulation, the adsorption layer becomes more dense, structured, and contains only lithium and fluorine ions. No defects are observed on the nickel surface.

Figure 4 shows the simulated cell cut along the z coordinate. The remaining part contains two nickel layers and a spontaneously formed dense adsorption layer of lithium fluoride. It is clearly seen that fluorine anions are located in positions above the nickel atoms that form the nearest surface layer. Lithium cations occupy positions above nickel atoms from the second layer, which are highlighted in blue for convenience. The arrangement of lithium cations and fluorine anions on the nickel surface is characterized by the distance between the nearest Li-F pairs of the order of 2 Å, which is close to the distance between this pair in a lithium fluoride crystal at high temperatures.

The adsorption layer formed at the very beginning of the simulation is a fairly dynamic structure. As noted earlier, sodium and potassium cations are replaced over time by lithium cations. At the same time, most of the fluorine anions continue to exchange with the melt

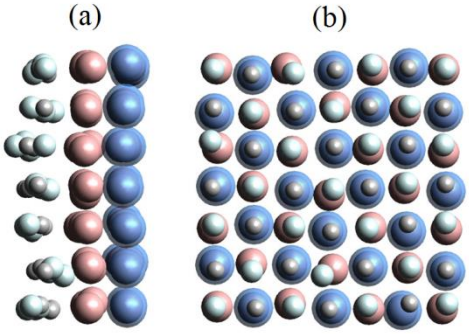

Figure 4 A fragment of the instantaneous configuration of the Ni - FLiNaK system at T = 800 K. The second layer of nickel, located farther from the interface, is highlighted in blue. (a) side view; (b) top view.

volume throughout the entire simulation time, while lithium cations leave the surface by an order of magnitude less frequently. This behavior correlates with the observed arrangement of ions on the surface of the nickel crystal lattice and can be explained from the standpoint of different Ni-Li^+ and Ni-F^- interaction energies. As can be seen from Table 1, the depth of the potential well for the Ni-Li^+ pair is approximately 25 % greater than for the Ni-F^- pair. In addition, the radius of the lithium cation of 0.816 Å is somewhat smaller than the radius of the fluorine anion of 1.179 Å [18], which serves as an additional factor for a more bound position of the lithium cation on the nickel surface.

After 15 ns of simulation, the distribution of ions near the nickel surface along the z axis, perpendicular to the interface plane, is shown in Figure 5. The ordinate shows the number of particles whose center of mass falls into the z coordinate with the interval of 0.05 Å. Data is averaged over time. The distributions presented in Figure 5 confirm that the adsorption layer is a separate and rather compact formation on the metal surface, with a thickness of the order of 2.6 Å. It is also seen that the adsorption layer consists of lithium and fluorine ions. Note that there is a small peak in the distribution of potassium cations at a distance of 5.2 Å from the metal surface. At the same time, the distribution curve for sodium cations has no features, since sodium, as well as potassium, are displaced from the adsorption layer at the considered temperature of 800 K.

When simulating a temperature of 1000 K for 15 ns, a dense adsorption layer is also formed at the beginning for several tens of picoseconds. Further exposure of the simulated cell at a temperature of T = 1000 K demonstrates the stability of the dense layer on the nickel surface over time. The main difference of the dense layer observed at T = 1000 K is that a small part of sodium cations remains in the formed two-dimensional structure on the metal surface. Figure 6(b) shows the distribution of lithium and sodium cations near the metal surface. Figure 6(a) also shows the instantaneous configuration of a part of the simulated cell consisting of two nickel layers and an adsorption layer after 15 nanoseconds. Figure 6 shows that the fraction of sodium cations remaining in the adsorption layer consist of several percent. The following reasoning could explain the observed effect. First, as the temperature increases, the dynamics of exchange between ions in the dense layer and the melt volume increases.

Now this applies not only to fluorine anions, but also lithium cations exchange more often with cations that are located in the space adjacent to the adsorption layer. Second, despite the fluoride eutectic contains only 11.5 mol. % of sodium fluoride, the calculated interaction

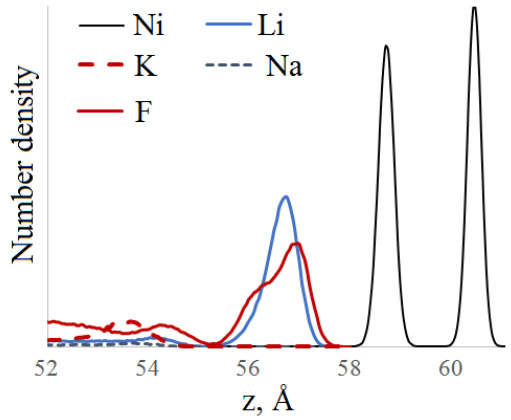

Figure 5 The distribution of ions and atoms along *z* axis at $T = 800$ K.

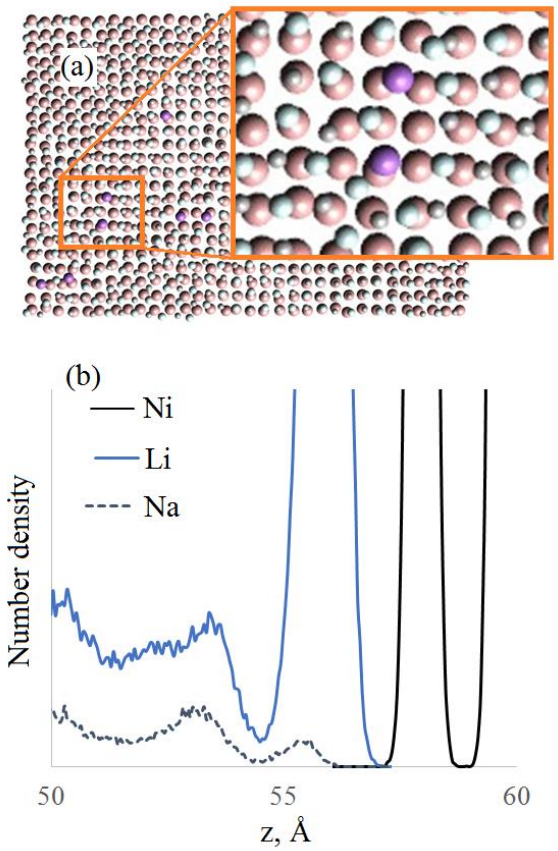

Figure 6 (a) Instantaneous configuration of a part of the Ni - FLiNaK system at $T = 1000$ K after 15 ns of simulation. A projection along the normal to the *z* axis is shown. Sodium cations are shown as pink circles. (b) Distribution of lithium, sodium and nickel atoms along the *z* axis at $T = 1000$ K.

parameters for sodium cations (see Table 1) with nickel atoms demonstrate the greatest depth of the potential well in comparison with other ions. While the structure of a two-dimensional layer of lithium fluoride on the surface is still stable, lithium cations become more mobile; therefore, some of their positions can be occupied by the sodium cation without breaking the symmetry in general.

3.2. $T = 1200$ K

Simulation of a two-phase Ni - FLiNaK system at $T = 1200$ K shows qualitatively new results. Figure 7 delivers the distribution functions of melt ions and nickel atoms after 15 nanoseconds of simulation.

An increase in temperature leads to a significant decrease in the stability of the adsorbed layer, as can be seen from the more diffuse nature of the distributions in Figure 7. Although there are still the large (as compared to the melt-averaged values) concentrations of lithium and fluorine ions near the metal surface, the stable two-dimensional structure is not formed. In addition, a peak was found on the distribution curve of nickel atoms in the region that goes beyond the nominal surface of the metal. Figure 8 shows the instantaneous configuration of two nickel surface layers after 15 nanoseconds of simulation at $T = 1200$ K.

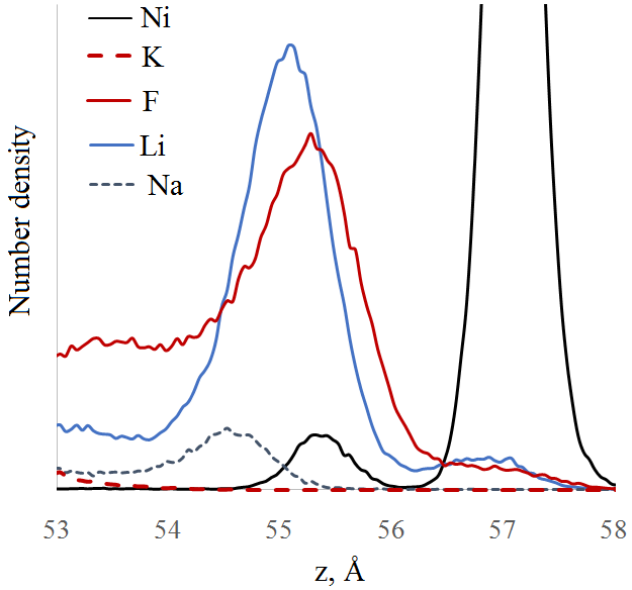

Figure 7 Distribution of melt ions and nickel atoms along the *z* axis at one of the interphase boundaries at $T = 1200$ K.

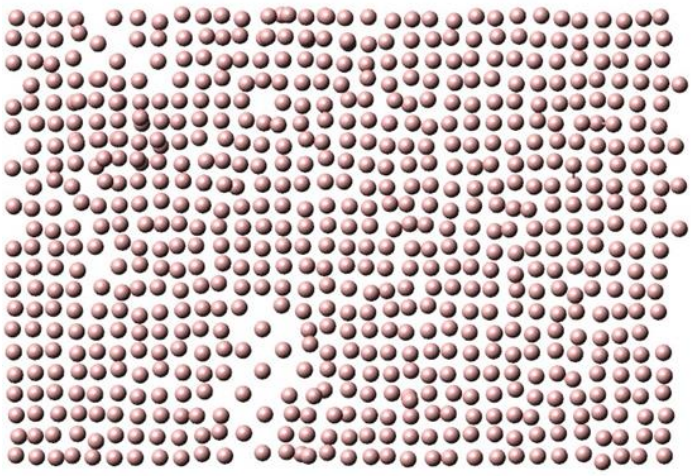

Figure 8 Instantaneous configuration of two nickel surface layers after 15 ns at $T = 1200$K.

Nickel atoms form point defects and various asymmetric structures on the surface, as evidenced by a small peak in the distribution curve of nickel atoms at z = 55.4 Å. As a result, the formed vacancies in the metal lattice to be filled with smaller lithium and fluorine ions, as can be seen in Figure 7. After 15 ns of simulations, the number of lithium and fluorine ions in the first nickel layer is several tens, while few ions approaching even the second nickel layer. Note that the temperature here is more than 500 K below the melting point of nickel. As known, the effects of premelting, including the intense formation of point defects in the crystal lattice, are observed within tens of Kelvin before melting temperature [19]. In our case, the defect formation in the surface layers of the metal long before the melting point could be connected with the presence of the melt.

3.3. Final remarks

At temperatures of 800 K and 1000 K, when a dense adsorption layer is formed on the surface, consisting mainly of two-dimensional lithium fluoride, nickel atoms are located at most part in the sites of the crystal lattice. As the temperature rises to 1200 K, the balance between the increasing thermal motion and the energy of pair interaction shifts toward the destruction of the structured two-dimensional layer on the metal surface. As a result, degradation of nickel surface layers is observed long before its melting point.

In this study, we aimed to investigate the possible mechanisms that lead to the stability of nickel in aggressive media of molten fluorides at temperatures available in most experiments. Therefore, the simulation time was limited to 15 nanoseconds. This time turned out to be enough to demonstrate the key phenomena and collect statistics. Issues related to the study of electrochemical corrosion of nickel with the participation of oxygen are beyond the scope of this work and cannot be studied using classical molecular dynamics in the approximation of the pair interaction model without description of chemical reactions.

4. Conclusions

In this paper, the molten FLiNaK eutectic melt was simulated in coexistence with crystalline Ni metal in order to investigate the features of physical absorption at the interphase. To properly describe pairwise interactions between metal atoms and ions of the melt, an *ab initio* calculation of energies was performed with a consequent fitting of model potential to reproduce reference energy values. A classical pairwise approach allowed considering time evolution of relatively large ensemble during several nanoseconds. This, in turn, made it possible to observe detailed information on the structure and dynamics of the adsorption layers. Let us summarize the main results. At lower temperatures (800 and 1000 K), the adsorption layer is constructed of Li^+ and F^- ions predominantly. These ions form a two-dimensional plate with symmetry of LiF crystal slice. It can be assumed that chemical composition of the adsorbed layer is to a large extent caused by the value of Ni lattice constant that is commensurable with the lattice constant of LiF. At a higher temperature of 1200 K, the adsorbed layer significantly reduces ordering. Moreover, there are numerous defects occur in Ni crystal layers, which are close to the FLiNaK. It can be stated that vacancies in Ni are filled by Li^+ and F^- ions from the melt. In general, it can be said that the physical corrosion of Ni is happening at 1200 K. It is important to note that our model do not allow Ni atoms to become cations. Therefore, to properly describe the dynamics of the coexisting metal and melt at higher temperatures, the reactive force field is needed.

Supplementary materials

No supplementary materials are available.

Funding

This research had no external funding.

Acknowledgments

None.

Author contributions

Dmitry Zakiryanov: Data curation; Formal Analysis; Writing – Original draft.

Mikhail Kobelev: Conceptualization; Validation; Visualization; Writing – Original draft; Writing – Review & Editing

Conflict of interest

The authors declare no conflict of interest.

Additional information

Dmitry Zakiryanov, Author ID: 57190936802; Orcid: 0000-0003-2649-7871.

Mikhail Kobelev, Author ID: 6603014470; Web of Science ResearcherID: J-3455-2018.

References

1. Olson L, Sridharan K, Anderson M, Allen T, Nickel-plating for active metal dissolution resistance in molten fluoride

salts, J. Nucl. Mater., **411** (2011) 51–59. https://doi.org/10.1016/j.jnucmat.2011.01.032

2. Wang Y, Zhang S, Ji X, Wang P, et al., Material corrosion in molten fluoride salts, Int. J. Electrochem. Sci., **13** (2018) 4891–4900. https://doi.org/10.1016/10.20964/2018.05.33

3. DorMahammadi H, Pang Q, Murkute P, Arnadottir L, et al., Investigation of chloride-induced depassivation of iron in alkaline media by reactive force field molecular dynamics, Materials Degradation, **3** (2019) 19. https://doi.org/10.1038/s41529-019-0081-6

4. Dong C, Ji Y, Wei X, Xu A, et al., Integrated computation of corrosion: Modelling, simulation and applications, Corrosion Communications, **2** (2021) 8–23. https://doi.org/10.1016/j.corcom.2021.07.001

5. Rudenko A, Redkin A, Il'ina E, Pershina S, et al., Thermal conductivity of FLiNaK in a molten state, Materials, **15** (2022) 5603. https://doi.org/10.3390/ma15165603

6. Ghods P, Isgor OB, Brown JR, Bensebaa F, et al., XPS depth profiling study on the passive oxide film of carbon steel in saturated calcium hydroxide solution and the effect of chloride on the film properties, Appl. Surface Sci., **257** (2011) 4669–4677. https://doi.org/10.1016/j.apsusc.2010.12.120

7. Zakiryanov D, Kobelev M, Tkachev N, Melting properties of alkali halides and the cation-anion size difference: A molecular dynamics study, Fluid Phase Equil., **506** (2020) 112369. https://doi.org/10.1016/j.fluid.2019.112369

8. Zakiryanov DO, Applying the Born-Mayer model to describe the physicochemical properties of FLiNaK ternary melt, Comp. Theor. Chem., **1219** (2023) 113951. https://doi.org/10.1016/j.comptc.2022.113951

9. Foiles SM, Baskes MI, Daw MS, Embedded-atom-method functions for the fcc metals Cu, Ag, Au, Ni, Pd, Pt, and their alloys, Phys. Rev. B, **33** (1986) 7983–7991. https://doi.org/10.1103/PhysRevB.33.7983

10. Morse PM, Diatomic molecules according to the wave mechanics. II. Vibrational levels, Phys. Rev., **34** (1929) 57–64. https://doi.org/10.1103/PhysRev.34.57

11. Latorre CA, Ewen JP, Gattinoni C, Dini D, Simulating surfactant – iron oxide interfaces: From density functional theory to molecular dynamics, J. Phys. Chem. B, **123** (2019) 6870–6881. https://doi.org/10.1021/acs.jpcb.9b02925

12. Guymon CG, Rowley RL, Harb JN, Wheeler DR, Simulating an electrochemical interface using charge dynamics, Cond. Matter Phys., **8(2)** (2005) 335–356. https://doi.org/10.5488/CMP.8.2.335

13. Adamo C, Barone V, Toward reliable density functional methods without adjustable parameters: The PBE0 model, J. Chem. Phys., **110** (1999) 6158–6170. https://doi.org/10.1063/1.478522

14. Grimme S, Antony J, Ehrlich S, Krieg H, A consistent and accurate ab initio parametrization of density functional dispersion correction (DFT-D) for the 94 elements H-Pu, J. Chem. Phys., **132** (2010) 154104. https://doi.org/10.1063/1.3382344

15. Weigend F, Accurate coulomb-fitting basis sets for H to Rn, Phys. Chem. Chem. Phys., **8** (2006) 1057–1065. https://doi.org/10.1039/B515623H

16. Nosé S, Constant temperature molecular dynamics methods, Prog. Theor. Phys. Supp., **103** (1991) 1–46. https://doi.org/10.1143/PTPS.103.1

17. Thompson HM, Aktulga R, Berger DC, Bolintineanu WM, et al., LAMMPS – a flexible simulation tool for particle-based materials modeling at the atomic, meso, and continuum scales, Comp. Phys. Comm., **271** (2022) 10817. https://doi.org/10.1016/j.cpc.2021.108171

18. Fumi FG, Tosi MP, Ionic sizes and born repulsive parameters in the NaCl-type alkali halides – I The Huggins-Mayer and Pauling forms, J. Phys. Chem. Solids., **25** (1964) 31–43. https://doi.org/10.1016/0022-3697(64)90159-3

19. Cahn R, Crystal defects and melting, Nature, **273** (1978) 491–492. https://doi.org/10.1038/273491b0